

Generalized Interference Detection Scheme in Heterogeneous Low Power Wide Area Networks

Naoki Aihara¹ , Koichi Adachi^{1*} , Osamu Takyu^{2*} , Mai Ohta^{3*}, and Takeo Fujii^{1*}

¹Advanced Wireless and Communication Research Center, The University of Electrocommunications, Tokyo 182-8585, Japan

²Department of Electrical and Computer Engineering, Shinshu University, Nagano 380-8553, Japan

³Department of Electronics and Computer Science, Fukuoka University, Fukuoka 814-0180, Japan

*Member, IEEE

Manuscript received April 22, 2020; accepted April 27, 2020. Date of publication May 6, 2020; date of current version May 29, 2020.

Abstract—Resource allocation under massive connectivity is one of the most important research topics due to widespread Internet-of-Things and machine-to-machine communication. Since multiple systems share the same frequency band due to the scarcity of frequency spectrum, resource allocation that takes into account the intersystem interference is essential. In this letter, an interference detection scheme that detects the change of the intersystem interference state is proposed. The proposed scheme is based on density ratio estimation using the available information at the resource controller. For change detection, the controller generates standard samples and test samples. Estimating the density ratio between test and standard samples enables the controller to detect change of the intersystem interference state. Under long-range wide area networks and a wireless-sensor utility network coexisting environment, the numerical results elucidate that the proposed scheme can improve average packet delivery rate by 10% compared to the system without interference detection.

Index Terms—Sensor networks, frequency allocation, interference detection, low power wide area network (LPWAN), long-range wide area networks (LoRaWAN), resource allocation.

I. INTRODUCTION

Low power consumption communication is becoming more important due to the emerge of the Internet-of-Things (IoT) [1]. The long-range wide area network (LoRaWAN) is one of the promising network architectures for low power wide area networks. LoRaWAN provides low power consumption and long-range communication at the cost of data rate. Due to its simple medium access control protocol, packet collision happens more frequently as the number of LoRaWAN nodes increases. In existing works, spreading factor (SF) and frequency allocation scheme and the application of carrier sense multiple access with collision avoidance (CSMA/CA) has been proposed in order to avoid packet collision and mitigate mutual interference, respectively [2]–[5]. In [4], a Q-learning-based resource allocation scheme has been proposed.

So far, most research works assume that there is only one system in the communication area, i.e., the system of interest can occupy the frequency band exclusively. However, this assumption may not be appropriate in a realistic scenario. Since, in a more realistic scenario, multiple systems share the same frequency band, the performance of the system may be severely degraded by the intersystem interference. In [6], intersystem interference between LoRaWAN and wireless-sensor utility network (Wi-SUN) is experimentally evaluated under overlapping operating frequency bands. Therefore, efficient resource allocation and communication control schemes considering the effects of other systems are necessary. To take into account the intersystem interference, it is necessary to detect the intersystem interference state.

Up to now, roughly two types of research works have been done to detect the intersystem interference that is introduced by the other system. The first type is based on spectrum sensing [7], [8]. However, these researches are based on highly accurate spectrum sensing. Therefore, these schemes may not be suitable for the low power wide area system that accommodates low-cost devices. The second type is based on the error pattern of chips, symbols, and packets [9], [10]. However, these schemes rely on the assumption of typical interference systems, e.g., the same physical layer technology with the independent operator or wireless local area network. Therefore, these systems cannot be adopted for arbitrary systems. Moreover, most of the conventional schemes only consider detecting the appearance of intersystem interference. From the viewpoint of operational principles, it is preferable to detect the change of interference state, i.e., the appearance and the disappearance without any assumption, prior knowledge, and hardware enhancement.

An intersystem interference state change detection is developed in this letter for the efficient utilization of resources. Since the appearance and the disappearance of the intersystem interference change the state, the proposed scheme enables more efficient resource utilization. For the interference state change detection, a density ratio estimation [11] is applied. In order not to require training data, pseudo training data and test data are generated. Those data are obtained by sequentially generating a set of the sample values on each frequency channel. By this, the change of the intersystem interference state can be detected without any prior knowledge. Once the change of the intersystem interference state is detected, the frequency channel is reassigned to LoRaWAN nodes by relearning. The performance improvement brought by the proposed detection scheme is confirmed by computer simulation assuming the coexistence of LoRaWAN and Wi-SUN. It is shown that the average packet delivery rate (PDR) can be improved by about 10% by introducing the proposed intersystem interference state change detection and relearning.

Corresponding author: Naoki Aihara. (e-mail: aihara@awcc.uec.ac.jp).

Associate Editor: J. M. Corres.

Digital Object Identifier 10.1109/LENS.2020.2992723

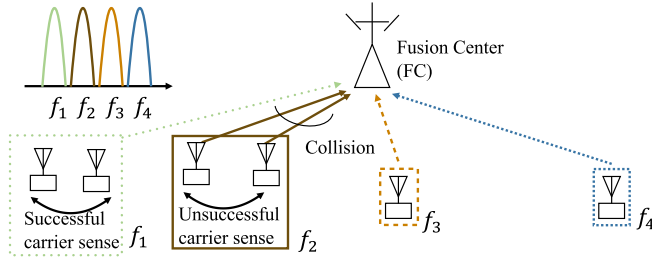


Fig. 1. LoRaWAN's frequency allocation model.

Table I. Data Rate and SNR/SIR Threshold.

SF	Bitrate [kbps] [2]	SNR threshold [dB] [2]	SIR threshold [dB] (w/ Wi-SUN) [15]	SIR threshold [dB] (w/o Wi-SUN) [6]
7	5.47	-6	-6	-11
8	3.13	-9	-9	-13
9	1.76	-12.5	-12.5	-16
10	0.98	-15.0	-16	-19
11	0.54	-17.5	-16	-22
12	0.29	-20.0	-16	-24

II. SYSTEM MODEL

In this letter, we assume the LoRaWAN and Wi-SUN coexisting scenario. Fig. 1 shows the LoRaWAN system considered in this letter. N LoRaWAN nodes (set \mathcal{N}) are randomly and uniformly distributed within a network area of $D \times D$ [km²]. A fusion center (FC) that controls LoRaWAN nodes and receives information from them is located at the center of the area. This FC can inform each LoRaWAN of available frequency channels regularly [12]. In total, K orthogonal frequency channels (set \mathcal{K}) are available. In this letter, FC allocates resource using a Q-learning based resource allocation scheme [4].

Each LoRaWAN node generates traffic of two types [13]. The first traffic is generated regularly at each LoRaWAN node following predetermined packet generation interval $T_{\text{interval},n}$ [s]. A random offset $T_{\text{offset},n} \sim \mathcal{U}[0, T_{\text{interval},n}]$ is assigned to LoRaWAN node n , where packet generation interval indicates application type in the communication area such as gas meter and water supply meter. The second traffic is generated when an event is detected. In this letter, an event occurs once at a random time in each epoch at a random position, and it propagates in the communication area with predetermined speed [13]. We assume the same packet size of N_{trans} [b] for these two traffic types.

LoRaWAN node n transmits packets with SF $S_n \in \{7, 8, 9, 10, 11, 12\}$. Each SF has its own data rate, signal-to-noise power ratio (SNR) threshold Γ_{SNR,S_n} , and signal-to-interference power ratio (SIR) threshold Γ_{SIR,S_n} . In this letter, it is assumed that each LoRaWAN node selects the SF that can maximize data rate while satisfying SNR threshold. If both SNR $\gamma_{\text{SNR},n}$ and SIR $\gamma_{\text{SIR},n}$ is above thresholds Γ_{SNR,S_n} and Γ_{SIR,S_n} , the packet from LoRaWAN node n is considered to be successfully received by the FC. For SIR threshold calculation, three thresholds are taken into account as $\Gamma_{\text{SIR},S_n} = \max(\Gamma_{\text{co}}, \Gamma_{\text{system}}, \Gamma_{\text{inter}})$, where $\max(\cdot)$ returns the maximum value of the arguments.

- 1) Co-SF Interference Γ_{co} : If there are nodes using the same SF as desired LoRaWAN node n , this interference needs to be considered. The SIR threshold Γ_{SF} is 6 [dB] [14].
- 2) Inter-SF Interference Γ_{inter} : If Wi-SUN interference exists, SIR threshold Γ_{inter} is selected from the middle column entitled “w/ Wi-SUN” in Table 1.

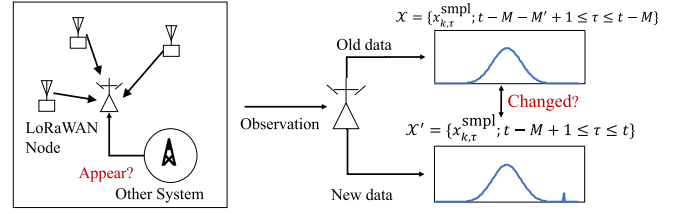


Fig. 2. Proposed model.

- 3) Wi-SUN Interference Γ_{system} : If neither intra-SF interference nor Wi-SUN interference exists, SIR threshold Γ_{intra} is selected from the right column entitled “w/o Wi-SUN” in Table 1.

A. Channel Model

The received signal power of LoRaWAN node n at FC is given as

$$P_{r,n} = P_{t,n} - P_{\text{pl}}(d_n) - \psi \quad (1)$$

where $P_{t,n}$ [dBm] is transmit power of LoRaWAN node n , $P_{\text{pl}}(d_n)$ [dB] is a path loss component, and ψ [dB] is a shadowing component. The pathloss component is given as

$$P_{\text{pl}}(d_n) = 10a \log_{10} d_n + b + 10c \log_{10} f_c \quad (2)$$

where d_n [km] is the distance between LoRaWAN node n and the FC, and f_c [MHz] is the carrier frequency. Propagation parameters a , b , and c are the coefficients for distance, offset, and frequency loss component, respectively [16].

B. Interference Model

The SNR and SIR for LoRaWAN node n are calculated as

$$\begin{cases} \gamma_{\text{SNR},n} = \frac{P_{r,n}}{A_{\text{noise}} P_{\text{noise}}} \\ \gamma_{\text{SIR},n} = \frac{P_{r,n}}{\sum_{n' \in \bar{\mathcal{N}}(n)} P_{r,n'} + P_{\text{int},k,n}} \end{cases} \quad (3)$$

In SNR calculation, A_{noise} is the noise figure and P_{noise} is the noise power. In SIR calculation, the first term of the denominator indicates the intrasystem interference that is the sum of received power of interfering LoRaWAN nodes at FC. $\bar{\mathcal{N}}(n)$ is the set of interfering LoRaWAN nodes that transmit packets using the same frequency channel with LoRaWAN node n simultaneously. The second term of the denominator indicates the intersystem interference. In this letter, we assume that Wi-SUN flips state {appear, disappear} at the state change time T_{int} . If Wi-SUN's state is “appear,” Wi-SUN packets interfere with LoRaWAN packets with power $P_{\text{int},k}$. We assume that $P_{\text{int},k}$ depends on i.i.d. log-normally distribution, i.e., $P_{\text{int},k} \sim e^{\mathcal{N}(\mu_k, \sigma_{\text{int}}^2)}$. Distribution parameters are empirically obtained with transmit power of 13 [dBm] [17].

III. PROPOSED SCHEME

Fig. 2 shows the proposed model. The controller detects the intersystem interference state changes from the observable data at the FC using a distribution change detection scheme, e.g., density ratio estimation. In this letter, the controller splits observed data into two exclusive sets and generates two different distributions. The first distribution is generated from relatively old observed data, and the second distribution is generated from relatively new observed data. If these distributions are different, the controller decides that the interference

state is changed. Although similar approaches are taken in the existing schemes [9], [10], these schemes assume the interference state before observation, e.g., the samples of distribution $p(x)$ are observed from the system without interference. No such assumption is required for the proposed scheme.

The proposed scheme has two advantages. First, it is not necessary to assume the interference state. Second, this scheme can detect the change of interference state, i.e., the appearance and the disappearance of the interference. This is because the proposed scheme does not assume the normal interference state.

A. Sequential Sample Set Generation

In this section, how to obtain the sample set from standard distribution $p(x)$ and that from test distribution $p'(x)$ is explained. The normalized number of successfully received packets, $x_{k,t}^{\text{smp1}}$, on frequency channel k during epoch t is used as a sample, which is obtained as

$$x_{k,t}^{\text{smp1}} = \frac{\sum_{n \in \mathcal{N}, k_n = k} D_{n,t}}{N_{k,t} \times T_{\text{epoch}}} \quad (4)$$

where $N_{k,t}$ is the number of LoRaWAN nodes allocated to frequency channel k during epoch t , i.e., $k_n = k$.

Let us denote the number of standard samples by M and that of test samples by M' , and further let us define standard sample set $\mathcal{X} = (x_{k,t-M}^{\text{smp1}}, \dots, x_{k,t-M'}^{\text{smp1}})$ and test sample set $\mathcal{X}' = (x_{k,t-M'}^{\text{smp1}}, \dots, x_{k,t-1}^{\text{smp1}})$ that are obtained as follows. Without loss of generality, let us consider the procedure at epoch t .

- 1) The observation data at epoch t , $x_{k,t-1}^{\text{smp1}}$ is obtained by (4).
- 2) Test sample set \mathcal{X}' is updated as

$$\mathcal{X}' \leftarrow \mathcal{X}' \setminus x_{k,t-M'}^{\text{smp1}} \cup x_{k,t-1}^{\text{smp1}}.$$

- 3) Standard sample set \mathcal{X} is updated as

$$\mathcal{X} \leftarrow \mathcal{X} \setminus x_{k,t-M}^{\text{smp1}} \cup x_{k,t-M'}^{\text{smp1}}.$$

- 4) The density ratio, $r(\mathcal{X}, \mathcal{X}')$, is obtained as

$$r(\mathcal{X}, \mathcal{X}') = \frac{p(\mathcal{X}')}{p(\mathcal{X})}$$

where $p(\mathcal{X})$ is a function to generate a probability distribution function from set \mathcal{X} .

- 5) If $r(\mathcal{X}, \mathcal{X}') > a_{\text{th}}$, then interference state is treated as changed.

B. ReLearning

Once the intersystem interference state is detected to be changed, the FC performs a Q-learning based wireless resource allocation proposed in [4]. Once the intersystem interference appears on a specific frequency channel, the system tries to avoid that frequency channel. On the other hand, once the intersystem interference disappears, the system tries to use the frequency channel previously contaminated by the intersystem interference.

IV. PERFORMANCE EVALUATION

The wireless system parameters and traffic parameters are derived from the Japanese parameter configuration of LoRaWAN, LoRaWAN AS923, from document [18] and radio law of Japan [19]. The node-FC shadowing is calculated by a spatially correlated shadowing model [20]. This component is expressed as a function of the location of LoRaWAN node n , i.e., $\psi(x_n, y_n)$. Between LoRaWAN nodes,

Table 2. Simulation Parameter.

Simulation area $D \times D$	2×2 [km ²]
Number of LoRaWAN nodes N	5000
Propagation coefficients (a, b, c)	(4.0, 9.5, 4.5)
Shadowing deviation σ	3.48 [dB]
Carrier Sense (CS) threshold Γ_{CS}	-80 [dB]
Inter-system interference parameters $(\mu, \sigma_{\text{int}})$	(-18.66, 1.73)
Wi-SUN system state change time T_{int}	225 [epoch]
Packet size N_{trans}	100 [bits]
Number of epochs for learning T (initial, relearning)	(200,200)
Number of Neural Network (NN) layers L	3
Number of neurons of hidden layer	10
Density ratio estimation parameters (h, a_{th})	(0.001, 10)
Number of standard samples M	5
Number of test samples M'	5

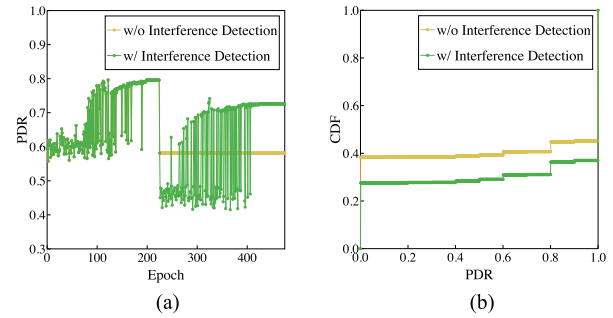


Fig. 3. PDR performance with appearing intersystem interference. (a) Learning process. (b) CDF of PDR.

shadowing is calculated using uncorrelated shadowing. Therefore, this component is expressed as the function of nodes index $\psi(n, q)$ where n and q are indices of nodes. In both situations, uncorrelated shadowing is based on log-normally distributed shadowing loss with zero-mean and standard deviation of σ [dB]. For learning parameters, the appropriate parameters are selected empirically, and we adopt stochastic gradient descent [21] as an optimizer and radial basis function kernel for calculation of basis function, which is given by

$$\phi_m(\mathbf{x}) = \exp\left(-\frac{\|\mathbf{x} - \mathbf{x}_m\|^2}{2h^2}\right). \quad (5)$$

Since most of the simulation parameters follow [4], only typical simulation parameters are shown in Table 2 due to the lack of space.

A. Simulation Results

For comparison, the PDR performance of the system without learning and that of [4] are shown. Since FC should send acknowledgment message to packets transmitted from LoRaWAN nodes as less as possible in order to satisfy the duty cycle recommendation [22], no retransmission protocol is introduced. Thus, PDR performance is selected as a performance metric to evaluate the reliable transmission in this letter. The performance of the system with the proposed interference detection is plotted by green-colored lines and that without is plotted by yellow-colored lines.

1) *Scenario 1. Interference Appearance:* In this scenario, the interference state is initially “disappearance,” and the interference appears at T_{int} . Fig. 3(a) shows how the proposed interference detection scheme can detect the change of the interference status. It can be seen from the figure that the PDR performance severely degrades if no interference detection is introduced. By introducing the proposed interference

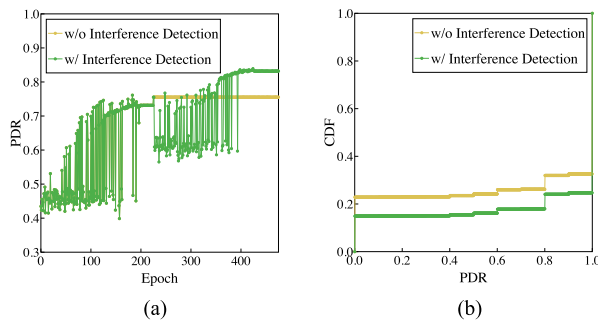


Fig. 4. PDR performance with disappearing intersystem interference. (a) Learning process. (b) CDF of PDR.

detection scheme, the system can successfully detect the change of the interference state and execute the relearning process. Thus, it can significantly improve the PDR performance. Although the PDR performance degrades during relearning process due to additional learning overhead, the proposed scheme can efficiently allocate the frequency channels by avoiding the frequency channel contaminated by the intersystem interference. This performance improvement is also clear in Fig. 3(b), where the cumulative distribution function (CDF) of PDR is shown. In this scenario, the proposed scheme can improve the average PDR performance by about 10%. This improvement is seen from Fig. 3(a) after $t = 475$ [epoch].

2) *Scenario 2. Interference Disappearance:* In this scenario, the interference state is initially “appearance,” and the interference disappears at T_{int} . Fig. 4(a) shows how the interference detection scheme can also detect the disappearance of the interference status. It can be seen from the figure that the PDR performance slightly improves if no interference detection is introduced. The available frequency resources are not efficiently utilized. By introducing the proposed interference detection scheme, the system can successfully detect the change of the interference state and execute the relearning process. Thus, it can significantly improve the PDR performance. Although it takes additional learning overhead, the proposed scheme can efficiently utilize the frequency channel previously contaminated by the intersystem interference. This performance improvement is also shown in Fig. 4(b). In this situation, the proposed scheme can improve the average PDR performance by about 8%.

V. CONCLUSION

In this letter, we proposed a detection scheme of the state of the intersystem interference to enable efficient frequency channel allocation. This detection scheme estimates the interference state based on the density ratio estimation by sequentially generating pseudo data sets. Thus, FC can detect the change of intersystem interference state without any prior assumption and knowledge. Computer simulation results have shown that the proposed scheme can detect the change of interference state and can improve average PDR performance by about 10% compared to the system without the detection of the intersystem interference state.

ACKNOWLEDGMENT

This research and development work was supported by MIC/SCOPE 175104004.

REFERENCES

- [1] U. Raza, P. Kulkarni, and M. Sooriyabandara, “Low power wide area networks: An overview,” *IEEE Commun. Surv. Tut.*, vol. 19, no. 2, pp. 855–873, Second quarter, 2017.
- [2] L. Amichi, M. Kaneko, N. E. Rachkidy, and A. Guitten, “Spreading factor allocation strategy for LoRa networks under imperfect orthogonality,” in *Proc. IEEE Int. Conf. Commun.*, 2019, pp. 1–7.
- [3] J. T. Lim and Y. Han, “Spreading factor allocation for massive connectivity in LoRa systems,” *IEEE Commun. Lett.*, vol. 22, no. 4, pp. 800–803, Apr. 2018.
- [4] N. Aihara, K. Adachi, O. Takyu, M. Ohta, and T. Fujii, “Q-learning aided resource allocation and environment recognition in LoRaWAN with CSMA/CA,” *IEEE Access*, vol. 7, no. 1, pp. 152 126–152 137, 2019.
- [5] J. Ortin, M. Cesana, and A. Redondi, “Augmenting LoRaWAN performance with listen before talk,” *IEEE Trans. Wireless Commun.*, vol. 18, no. 6, pp. 3113–3128, Jun. 2019.
- [6] C. Orfanidis, L. M. Feeney, M. Jacobsson, and P. Gunningberg, “Investigating interference between LoRa and IEEE 802.15.4 G networks,” in *Proc. Int. Conf. Wireless Mobile Comput., Netw. Commun.*, 2017, pp. 1–8.
- [7] A. J. Coulson, “Spectrum sensing using hidden Markov modeling,” in *Proc. IEEE Int. Conf. Commun.*, 2009, pp. 1–6.
- [8] A. Badawy, A. E. Shafie, and T. Khattab, “On the performance of quickest detection spectrum sensing: The case of cumulative sum,” *IEEE Commun. Lett.*, vol. 24, no. 4, pp. 749–743, Apr. 2020.
- [9] F. Barac, S. Caiola, M. Gidlund, E. Sisinni, and T. Zhang, “Channel diagnostics for wireless sensor networks in harsh industrial environments,” *IEEE Sensors J.*, vol. 14, no. 11, pp. 3983–3995, Nov. 2014.
- [10] C. H. Uy, C. Bernier, and S. Charbonnier, “Design of a low complexity interference detector for LPWA networks,” in *Proc. IEEE Int. Instrum. Meas. Technol. Conf.*, 2019, pp. 1–6.
- [11] T. Kanamori, S. Hido, and M. Sugiyama, “A least-squares approach to direct importance estimation,” *J. Mach. Learn. Res.*, vol. 10, pp. 1391–1445, 2009.
- [12] LoRa Alliance Technical Committee, “LoRaWAN 1.1 Specification,” 2017. [Online]. Available: <https://loro-alliance.org/resource-hub/lorawan-specification-v11>
- [13] V. Gupta, S. K. Devar, N. H. Kumar, and K. P. Bagadi, “Modelling of IoT traffic and its impact on LoRaWAN,” in *Proc. IEEE Global Commun. Conf.*, 2017, pp. 1–6.
- [14] C. Goursaud and J. M. Gorce, “Dedicated networks for IoT: PHY / MAC state of the art and challenges,” *EAI Endorsed Trans. Internet Things*, vol. 1, no. 1, pp. 1–12, 2015.
- [15] D. Croce, M. Gucciardo, S. Mangione, G. Santaromita, and I. Tinnirello, “Impact of LoRa imperfect orthogonality: Analysis of link-level performance,” *IEEE Commun. Lett.*, vol. 22, no. 4, pp. 796–799, Apr. 2018.
- [16] ITU-R, “Propagation data and prediction methods for the planning of short-range outdoor radiocommunication systems and radio local area networks in the frequency range 300 MHz to 100 GHz,” 2017. [Online]. Available: <https://www.itu.int/rec/R-REC-P.1411/en>
- [17] H. Harada, K. Mizutani, J. Fujiwara, K. Mochizuki, K. Obata, and R. Okumura, “IEEE 802.15.4 g based Wi-SUN communication systems,” *IEICE Trans. Commun.*, vol. E100-B, no. 7, pp. 1032–1043, 2017.
- [18] LoRa Alliance Technical Committee, “LoRaWAN regional parameters v1.1 REV A,” 2018. [Online]. Available: <https://loro-alliance.org/resource-hub/lorawan-regional-parameters-v11ra>
- [19] ARIB, “920 MHz-band telemeter, telecontrol and data transmission radio equipment,” 2012. [Online]. Available: https://www.arib.or.jp/english/html/overview/doc/5-STD-T108v1_0-E1.pdf
- [20] H. Claussen, “Efficient modelling of channel maps with correlated shadow fading in mobile radio systems,” in *Proc. IEEE Int. Symp. Personal, Indoor Mobile Radio Commun.*, 2005, pp. 512–516.
- [21] C. M. Bishop, *Pattern Recognition and Machine Learning*. Berlin, Germany: Springer, 2010.
- [22] V. D. I. Vincenzo, M. Heusse, and B. Tourancheau, “Improving downlink scalability in LoRaWAN,” in *Proc. IEEE Int. Conf. Commun.*, 2019, pp. 1–6.